ELSEVIER

Polymer 43 (2002) 3635–3645

polymer

www.elsevier.com/locate/polymer

A computational study of iron-based Gibson–Brookhart catalysts for the copolymerisation of ethylene and 1-hexene

J. Ramos[a], V. Cruz[b], A. Muñoz-Escalona[a], J. Martínez-Salazar[a,*]

[a]*GIDEM, Instituto de Estructura de la Materia, CSIC, Serrano 113-bis-119-121-123, 28006 Madrid, Spain*
[b]*C.T.I., CSIC, Pinar 19, 28006 Madrid, Spain*

Received 23 August 2001; received in revised form 2 November 2001; accepted 22 February 2002

Abstract

A combined QM/MM study of the ethylene/1-hexene copolymerisation with bisiminepyridine iron(II) is presented. It has been found experimentally that these catalysts do not copolymerise ethylene with 1-hexene. Based on the mechanism of propagation and termination processes proposed by Deng et al., we have performed calculations for the ethylene and 1-hexene monomers in order to give a suitable explanation to the experimental findings. The propagation reaction is divided into two fundamental steps: the backside monomer capture and the backside monomer insertion. The energy barriers for these steps are, respectively, 2.11 and 0.59 kcal/mol for the ethylene monomer and 6.62 and 5.43 kcal/mol for 1-hexene. Additionally, the backside π-complex formation for 1-hexene is an endothermic process by 0.72 kcal/mol. Therefore, the ethylene propagation reaction is very favourable as compared to the 1-hexene propagation. In the same way, the termination reaction is also divided into two elementary steps: the frontside monomer capture and the β-hydrogen transfer steps. The associated energy barriers for these two processes are, respectively, 5.83 and 6.55 kcal/mol for the ethylene monomer and 6.03 and 8.38 kcal/mol for 1-hexene. So, the differences between the rate-limiting step of the propagation and termination energy barriers are 4.44 kcal/mol for the ethylene and 1.76 kcal/mol for the 1-hexene monomer. These facts are in good agreement with concurrent experimental results. Furthermore, the role of the bulky ancillary ligands has been analysed. © 2002 Published by Elsevier Science Ltd.

Keywords: Iron(II)-bisiminepyridine catalysts; Ethylene/1-hexene copolymerisation; Homogeneous catalysis

1. Introduction

Metallocene complexes based on group IV metals as catalysts for the ethylene and α-olefins polymerisation have been used for almost 20 years [1–4]. They have been extensively studied by both experimental [1–4] and theoretical [5–16] techniques. Modifications of the classical metallocene complexes have been equally developed as an alternative route for polymerisation catalysts [17–19]. Some non-metallocene catalysts based on Zr and Ti have also been studied recently due to their ease of preparation in comparison to other metallocene catalysts [20–23].

In order to extend the range of new polymeric materials, considerable effort has been devoted to the discovery of new families of catalysts. More recently, diimine nickel (II) complexes synthesised by Brookhart's group and bisimine pyridine iron (II) complexes by the groups of Gibson and Brookhart have also been used for olefin polymerisation.

Diimine nickel (II) complexes have been broadly studied as an effort to avoid patent litigation in the metallocene catalysts area [24–27]. In order to clarify the polymerisation mechanisms of these catalysts considerable attention have been paid to theoretical calculations [28–37]. These catalysts possess the advantage that through small variations of pressure, temperature and ligand substituents they produce ethylene homopolymer with a hierarchy of architectures varying from highly branched, completely amorphous material to linear and semicrystalline, high-density products [24–26]. Additionally, they are capable of copolymerising ethylene and propylene with polar-functionalised vinyl monomers [27].

The idea that the late transition metal chelate complexes could polymerise α-olefins has stimulated the search for extending the range of organometallic complex catalysts. Furthermore, it is very interesting that the structure of the ancillary ligands attached to the metal centre could exert strong influence over the polymer properties. These facts have motivated the development of bulky tridentate bisiminepyridine complexes of iron and cobalt as catalysts for α-olefins polymerisation [38–41]. To our best knowledge,

* Corresponding author. Tel.: +34-91-561-68-00; fax: +34-91-564-55-57.
E-mail address: jmsalazar@iem.cfmac.csic.es (J. Martínez-Salazar).

0032-3861/02/$ - see front matter © 2002 Published by Elsevier Science Ltd.
PII: S0032-3861(02)00174-X

only two theoretical studies on these catalysts have been so far reported [42,43]. Deng et al. established for the first time the key steps of the mechanism for the ethylene polymerisation with iron (II)-bisiminepyridine catalyst using the QM(DFT)/MM approximation. The most important conclusions were: (i) the cationic iron(II) alkyl resting state adopts an axial conformation, (ii) chain propagation reaction starts through the backside approach of ethylene from the axial plane, the rate-determining step being the capture of ethylene, (iii) the chain termination path is β-H transfer from the polymer chain to the incoming monomer from the frontside axial face and (iv) chain propagation and termination occurs on the singlet potential electronic surface [43]. Later on, Griffiths et al. performed B3LYP calculation for the first ethylene insertion into the iron catalyst. They found the energy barrier associated with the first insertion to be very low (around of 2.5 kcal/mol) [42]. Therefore, it would be expected that these catalysts are more active than the Cp_2ZrCl_2 metallocene catalyst, where higher energy barriers of about 4–8 kcal/mol have been reported [9,11–13,16].

On the other hand, due to the fact that the copolymerisation of ethylene with high α-olefins comonomers is an important industrial process for the control of the densities of the produced polymers, it is very interesting to explore the capability of these novel catalysts for this type of reactions. It has been experimentally found that by using the bisiminepyridine iron catalyst it is very difficult to copolymerise ethylene with 1-hexene as a comonomer.[1] This represents a very conspicuous difference between metallocene and bisiminepyridine iron-based catalysts.

The aim of this work, it is to perform a theoretical study of the ethylene and 1-hexene polymerisation processes in order to give a suitable explanation of the earlier experimental findings. Thus, we have based our calculations on the mechanism proposed by Deng et al. [43]. Although these authors have already studied the homopolymerisation of ethylene, we do perform in this work similar calculation in order to compare this result with the copolymerisation of ethylene with 1-hexene in a consistent manner.

2. Computational methods

All calculations have been performed with the ADF package [44]. The QM/MM approximation due to Maseras–Morokuma [45] and implemented by Ziegler et al. into ADF [46] has been used in this work. The Scheme 1 displays the MM and QM subsystems partition for the bisiminepyridine-Fe(II) catalyst used in the present work. It is worthwhile to mention that the 1-hexene is not completely integrated into the QM subsystem, but only the first three carbon atoms are included. The rest of the comonomer is included in the MM part. This model is able to correctly describe the electronic and steric features of the 1-hexene

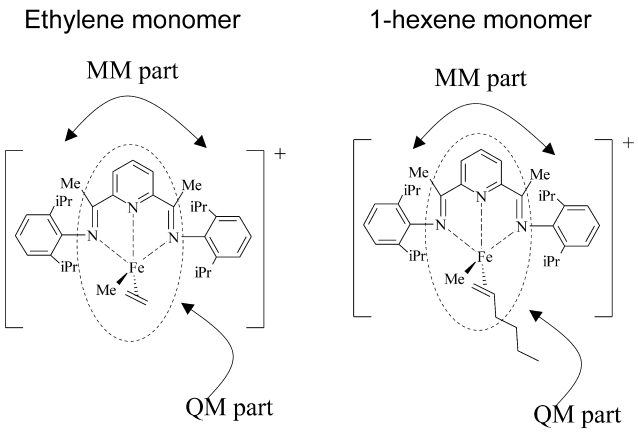

Scheme 1.

comonomer. Indeed, we have performed some calculations incorporating the complete 1-hexene molecule into the QM part obtaining very similar results for the two cases.[2]

In the framework of this approximation the total energies ($E_{QM/MM}$) of the system are separated into two components: (i) Molecular mechanics energy (E_{MM}) that accounts only for steric effects, i.e. electrostatic interactions are not included. (ii) Quantum mechanics energy (E_{QM}) that takes into consideration the most important electronic effects. Therefore, the total energies ($E_{QM/MM}$) are given as follows:

$$E_{QM/MM} = E_{MM} + E_{QM}$$

In the calculation of the QM subsystem the BP86 method, involving local density approximation [47] but adding non-local corrections to exchange [48] and correlation [49] was used. The frozen core approximation is applied to the innermost atomic shells. For the iron atom the outermost atomic shells have been treated with a basis function containing triple-ζ basis set plus a polarisation function. For the rest of the atoms a basis function containing a double-ζ basis set plus a polarisation function has been employed for the valence shells [44]. The Tripos 5.2 force field, including parameters for the iron atom, was applied to the MM subsystem.

3. Results and discussion

The key steps for the propagation and termination mechanisms are displayed in Scheme 2. The construction of this scheme is based on the mechanism proposed by Deng et al. [43].

First of all, we would like to clarify some points of the

[1] Internal Report of Repsol-YPF 2000.

[2] For example, when only three atoms of 1-hexene were included into the QM subsystem the energy barrier for the 2,1 capture of 1-hexene was 6.62 kcal/mol, while the energy barrier of 6.03 kcal/mol was found when all-atoms of 1-hexene were taking into account. Additionally, the energy differences between adduct and π-complex were also calculated given 0.72 kcal/mol (for three atoms) and 0.85 kcal/mol (for all-atoms), respectively. It can be seen that similar results were obtained.

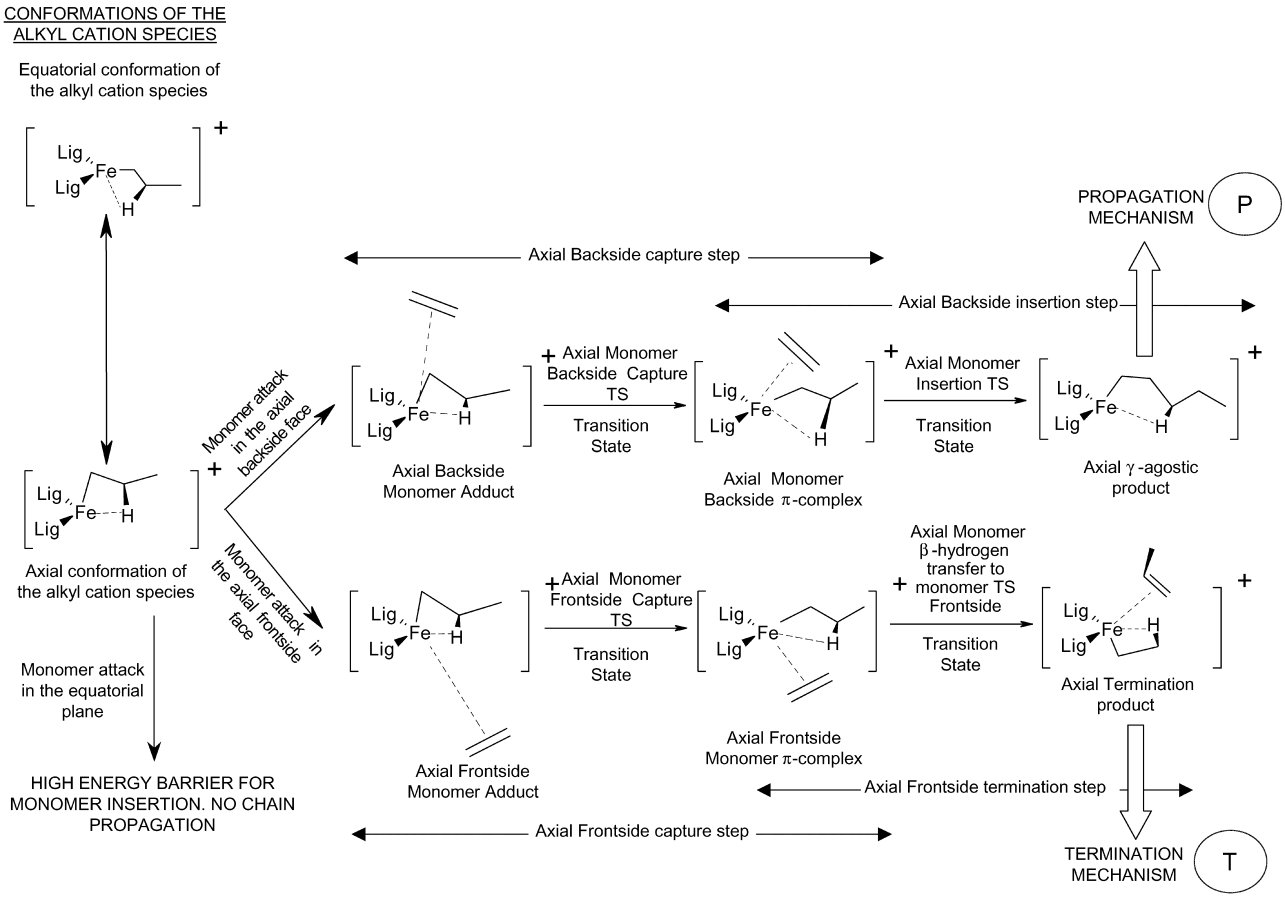

Scheme 2.

mechanism used in the present work. In Fig. 1(a) the Gibson–Brookhart catalyst has coordination around the metal centre close to a distorted square-pyramidal geometry [39]. In this coordination the chloride atoms, which will be replaced by methyl groups due to the cocatalyst action, are not equivalent. One of them is occupying the axial (apical) plane (Cl(1)) whereas the other one stays in the equatorial (basal) plane (Cl(2)). The equatorial plane contains the three

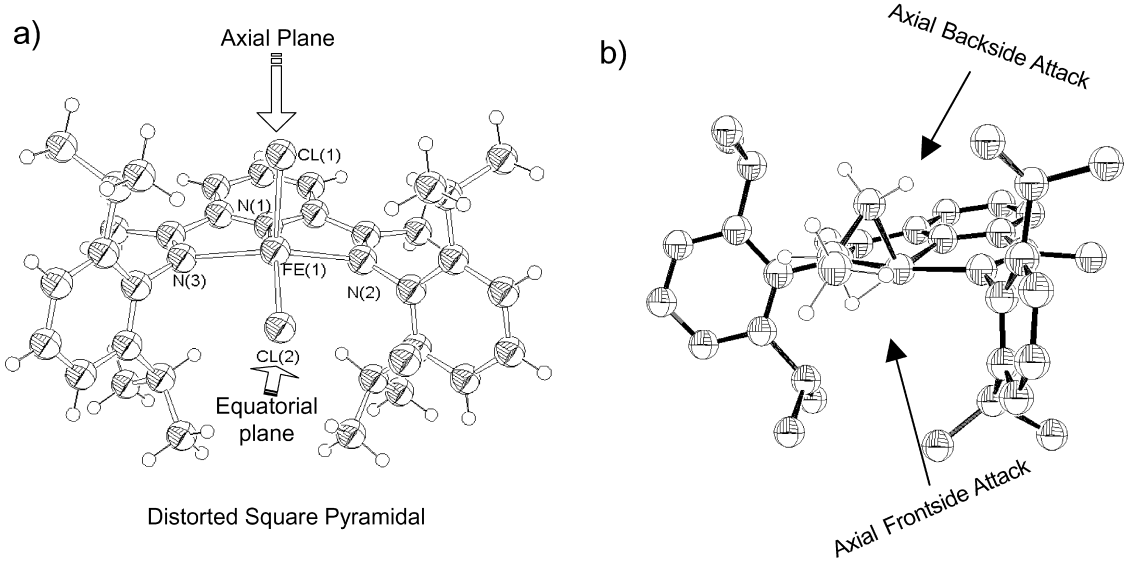

Fig. 1. (a) Experimental structure of the bis-iminepyridine iron(II) dichloride. Representation of the equatorial and the axial planes. (b) Definition of the axial backside and frontside attack into the axial conformation of the alkyl cation active species.

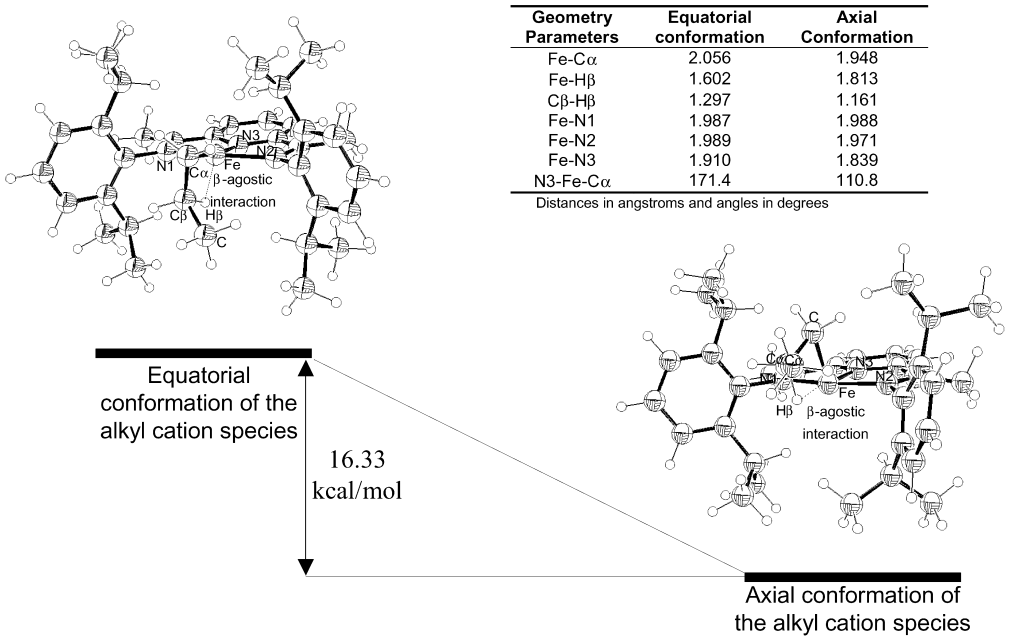

Geometry Parameters	Equatorial conformation	Axial Conformation
Fe-Cα	2.056	1.948
Fe-Hβ	1.602	1.813
Cβ-Hβ	1.297	1.161
Fe-N1	1.987	1.988
Fe-N2	1.989	1.971
Fe-N3	1.910	1.839
N3-Fe-Cα	171.4	110.8

Distances in angstroms and angles in degrees

Fig. 2. Optimised structures and relative energy for the equatorial and axial conformations of the alkyl cation species. Note that the N3 (nitrogen pyridyl), Fe and Cα atoms define the angle that gives an idea of the axial (near to 90°) or equatorial conformation (near to 180°).

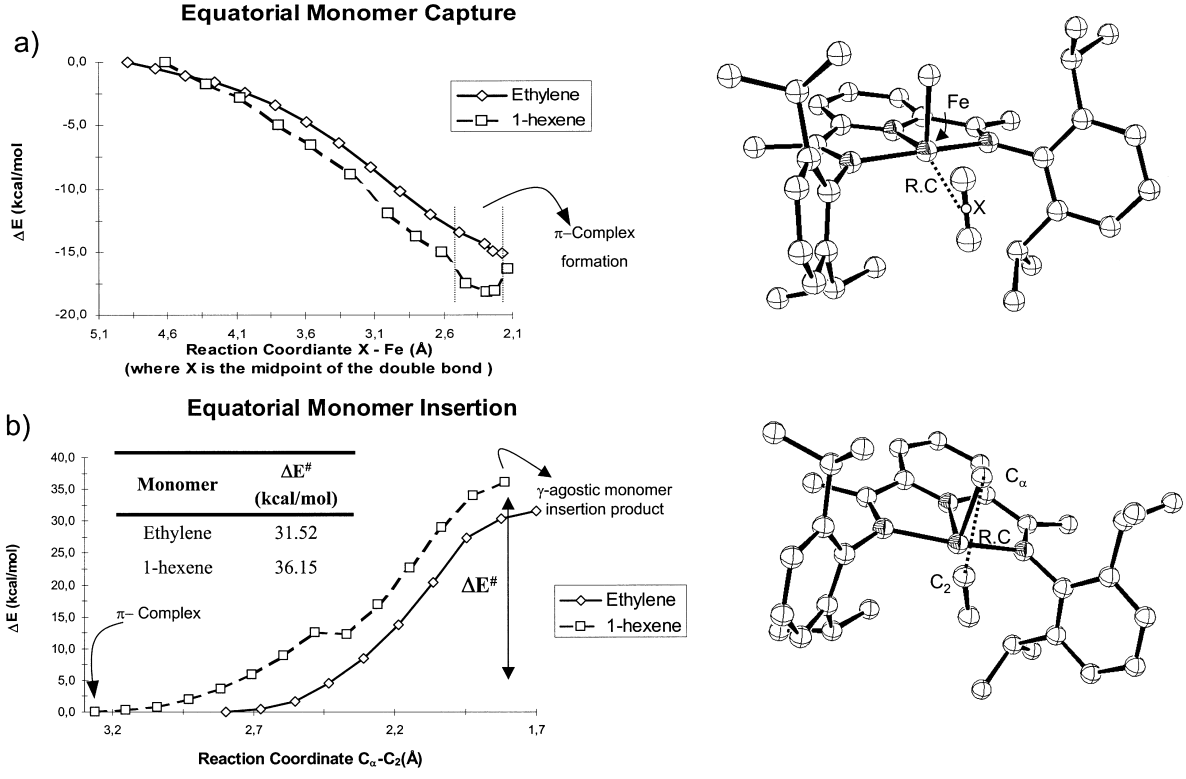

Fig. 3. (a) Energy profile of the capture process in the equatorial approach of the ethylene and 1-hexene monomer to the metal centre. The reaction coordinate was the distance between the double bond midpoint of the monomer and the iron atom. (b) Energy profile of the insertion process for the equatorial approach to the ethylene and 1-hexene monomer to the metal centre. The reaction coordinate was the distance between the C2 atom and the Cα atom. These profiles have been obtained using linear synchronous transit calculations.

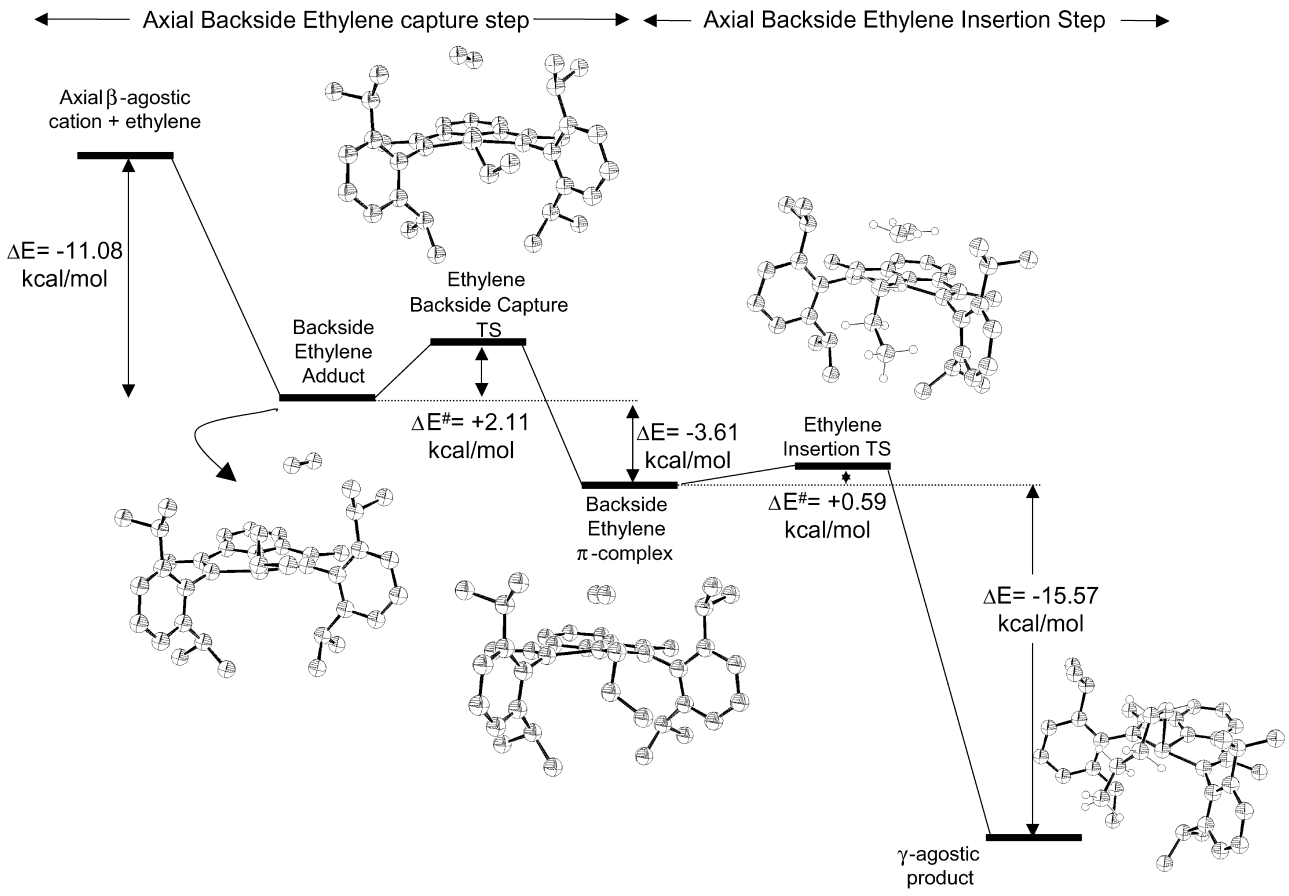

Fig. 4. Energy profile for the propagation reaction of the ethylene into the Fe–Cα bond. The propagation reaction corresponds to the axial backside approach of the ethylene to the metal centre (see text).

nitrogen atoms of the bisiminopyridine ligand and the chloride atom Cl(2). These two different planes (axial and equatorial) will define the physical sites where the incoming monomer could interact with the metal centre. Furthermore, in the axial plane the monomer can approach the metal centre from two opposite sites: the backside (*anti*) and the frontside (*syn*) faces (Fig. 1(b)). Here, in the backside face the incoming monomer approaches the back of the alkyl chain, whereas in the frontside face it approaches the front of the alkyl chain (Fig. 1(b), Scheme 2). The chain propagation reaction takes place by the axial backside approach mechanism, while the chain termination reaction occurs by axial frontside approach mechanism. Note that the frontside approach mechanism could never give rise to the monomer insertion because in this position the alkyl chain and the incoming monomer stay in opposite faces of the axial plane (up and down of the equatorial plane, respectively). Finally, the insertion of the monomer approaching the equatorial plane is very unlikely to occur, as it will be discussed later on.

The alkyl cationic species can adopt two conformations depending on the position of the alkyl chain: equatorial and axial conformations. As will be discussed later, only the axial conformation is active for the olefin polymerisation. Furthermore, the monomer can attack the axial active species by the equatorial or axial planes. The monomer attacking in the equatorial plane has a very high-energy barrier for the insertion reaction, so the propagation reaction cannot take place. Therefore only the incoming monomer approaching the alkyl cation species in the axial plane (back and front) could polymerise.

As proposed by Deng et al. [43], the propagation mechanism (P in Scheme 2) on the axial conformation of the alkyl cation species could be divided into two elementary steps: the axial backside capture and the axial backside insertion (Scheme 2). In the axial backside capture the monomer approaches the axial alkyl cation active species in order to make an adduct complex, which evolves to the typical π-complex through a transition state (monomer backside capture TS, in Scheme 2). Later on, in the axial backside insertion step, the π-complex progresses through the insertion transition state directly to the γ-agostic product.

Similarly, the termination mechanism (T in scheme 2) has been also divided into two elementary steps: the axial frontside capture and the axial frontside termination (see Scheme 2).

In the next sections, we will present the results of the calculations for all these steps.

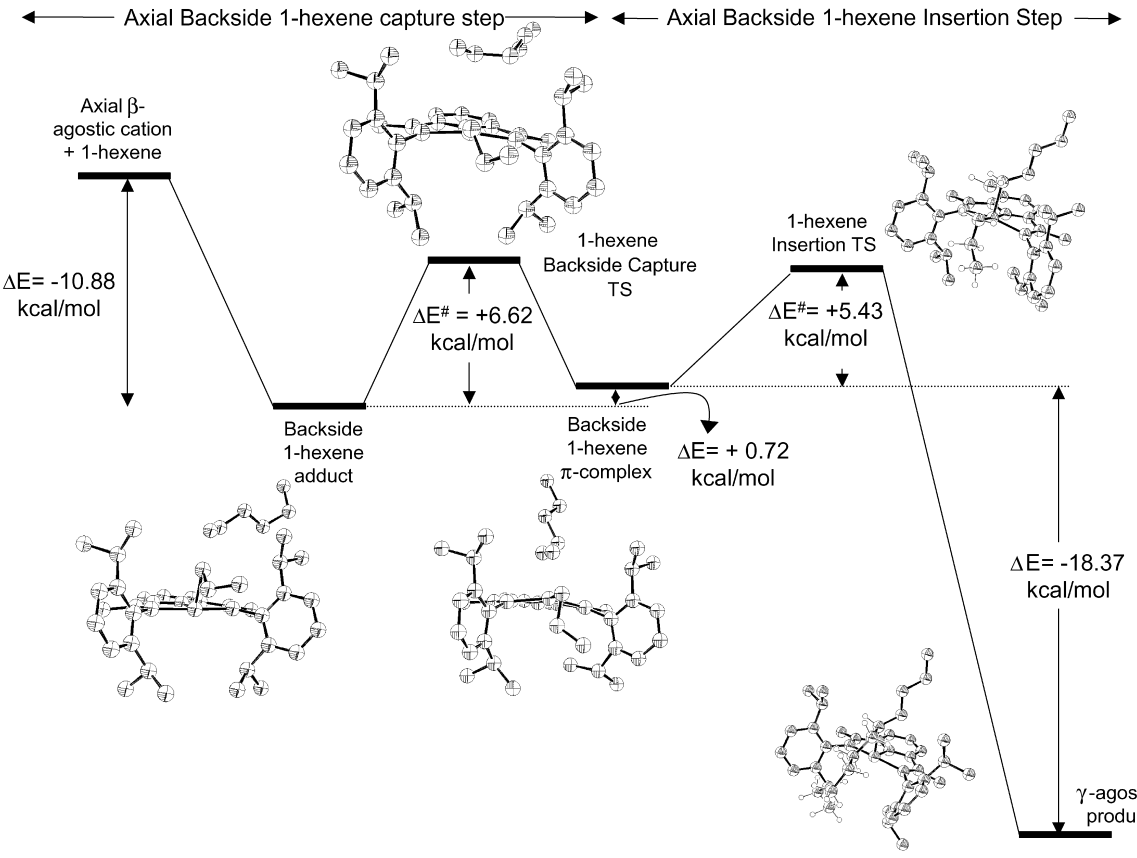

Fig. 5. Energy profile for the propagation reaction of the 1-hexene in 2,1 form into the Fe–Cα bond. The propagation reaction corresponds to the axial backside approach of the 1-hexene to the metal centre (see text for details).

3.1. Conformation of the cationic active species

Results obtained for the calculations of the two different conformations for the alkyl chain attached to the iron atom are given in Fig. 2. In this figure the most important geometry parameters and energies are also included. As it can be seen, the axial conformation is 16.33 kcal/mol more stable than the equatorial one.

Regarding geometry parameters taken from Fig. 2, the N3–Fe–Cα angle gives an idea of the chain position. Values close to 90° would be representative of an axial conformation while angle values close to 180° would be indicative of an equatorial conformation. It can be seen that the 110.8° angle corresponds to a nearly axial conformation while the angle 171.4° is near the equatorial one. In the equatorial conformation, it is observed that the β-agostic interaction is stronger than in the axial conformation as is also confirmed by the Fe–Hβ and CβHβ distances (1.602 and 1.297 Å for equatorial conformation and 1.813 and 1.161 Å for axial conformation). This result suggests that the axial position is the preferred one by this iron complex. That is one of the reasons why the axial conformation is more stable than the equatorial one, in good agreement with the results of Deng et al. [43].

3.2. Equatorial monomer insertion into axial alkyl cation conformation

Due to the fact that in the axial conformation the alkyl chain occupies the axial position, it could be assumed that the incoming monomer approaches the iron atom by the equatorial plane. Therefore, we have performed some linear transit calculations for the ethylene and 1-hexene insertions into the iron catalyst and the results are depicted in Fig. 3. This figure displays the reaction profiles for the ethylene and 1-hexene insertion processes, which have been divided again into two fundamental steps: (i) monomer capture and (ii) insertion reaction.

The profile for the monomer capture has been generated by varying the distance between the double bond midpoint of the monomer and the iron metal. As can be seen in Fig. 3(a) the approximation of the ethylene and 1-hexene monomers in the equatorial plane to the iron metal do not present any evidence of electronic energy barrier, which is an indication of an easy monomer capture for both ethylene and 1-hexene monomers.

Additionally, the insertion step is shown in Fig. 3(b). In this case, the profile was created by varying the distance between the C2 carbon atom of the monomer and the Cα carbon of the alkyl chain (Fig. 3(b)). Profiles obtained for

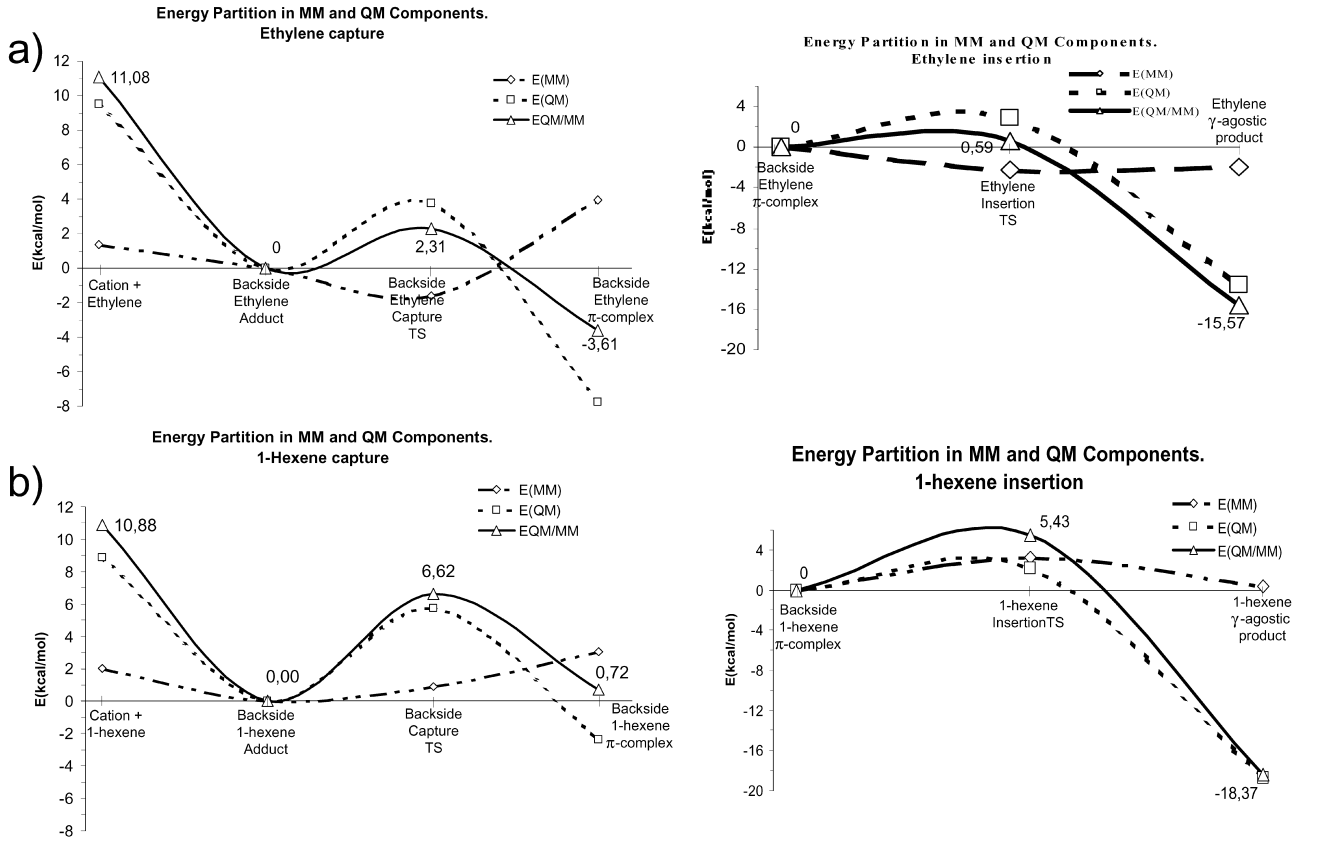

Fig. 6. $E_{QM/MM}$ partition in E_{MM} and $E_{QM\ pure}$ components (a) left, energy partition for the backside ethylene capture step (energies relatives to the backside ethylene adduct) and right, for the backside ethylene insertion step (energies relatives to the backside ethylene π-complex). (b) Left, energy partition for the backside 2,1 insertion 1-hexene capture step (energies relatives to the backside 1-hexene adduct) and right, for the backside 1-hexene insertion step (energies relatives to the backside 1-hexene π-complex).

ethylene and 1-hexene monomers are uphill (as can be seen in Fig. 3(b)) indicating a hard insertion process for both monomers. We have estimated that the energy barriers for ethylene and 1-hexene monomers are +31.52 and +36.15 kcal/mol, respectively. These energy barriers are very high in comparison with the experimental activities reported for these catalysts [38–40].

The earlier results indicate that the monomer insertion in the equatorial plane is not a favourable process for this catalyst. A possible explanation for the high energy barriers obtained for the monomer insertion in the equatorial plane can be found in the migratory insertion of the alkyl chain moving from the axial position to the equatorial one which is the least stable conformation. Similar explanations have been given by Deng et al. [43].

These results are in disagreement with the experimental findings that these catalysts are highly active for the ethylene polymerisation. For this reason, it could be deduced that the monomer insertion in the propagation reaction cannot take place in the equatorial plane. The only alternative is to consider that the monomer insertion takes place in the axial position. The results are given later.

3.3. Axial backside monomer insertion

In what follows we would like to point out that the ethylene and 1-hexene monomers both compete for the same kind of active centre.

In Figs. 4 and 5 the complete energy profiles for the insertion of ethylene and 2,1 insertion of 1-hexene in the axial plane of the bisiminepyridine-Fe (II) catalysts are given. The 1,2 insertion of 1-hexene will be discussed later. However, as it will be seen the 2,1 insertion is preferred over the 1,2 insertion.

It has been found that an adduct complex between the cationic catalyst species and the monomer, for both ethylene and 1-hexene monomers, is formed before the typical π-complex is reached. The ethylene and 1-hexene adducts are 11.08 and 10.88 kcal/mol, respectively, more stable than the separate reactants (β-agostic cation and monomer). Therefore, the ethylene adduct is only 0.2 kcal/mol more stable that the 1-hexene adduct.

The monomer adducts evolve through a transition state towards the intermediate π-complex, for both ethylene and 1-hexene monomers. The energy barrier for this process is 2.11 kcal/mol for ethylene monomer (Fig. 4) and 6.62 kcal/mol for 1-hexene (Fig. 5). Therefore, the ethylene capture is

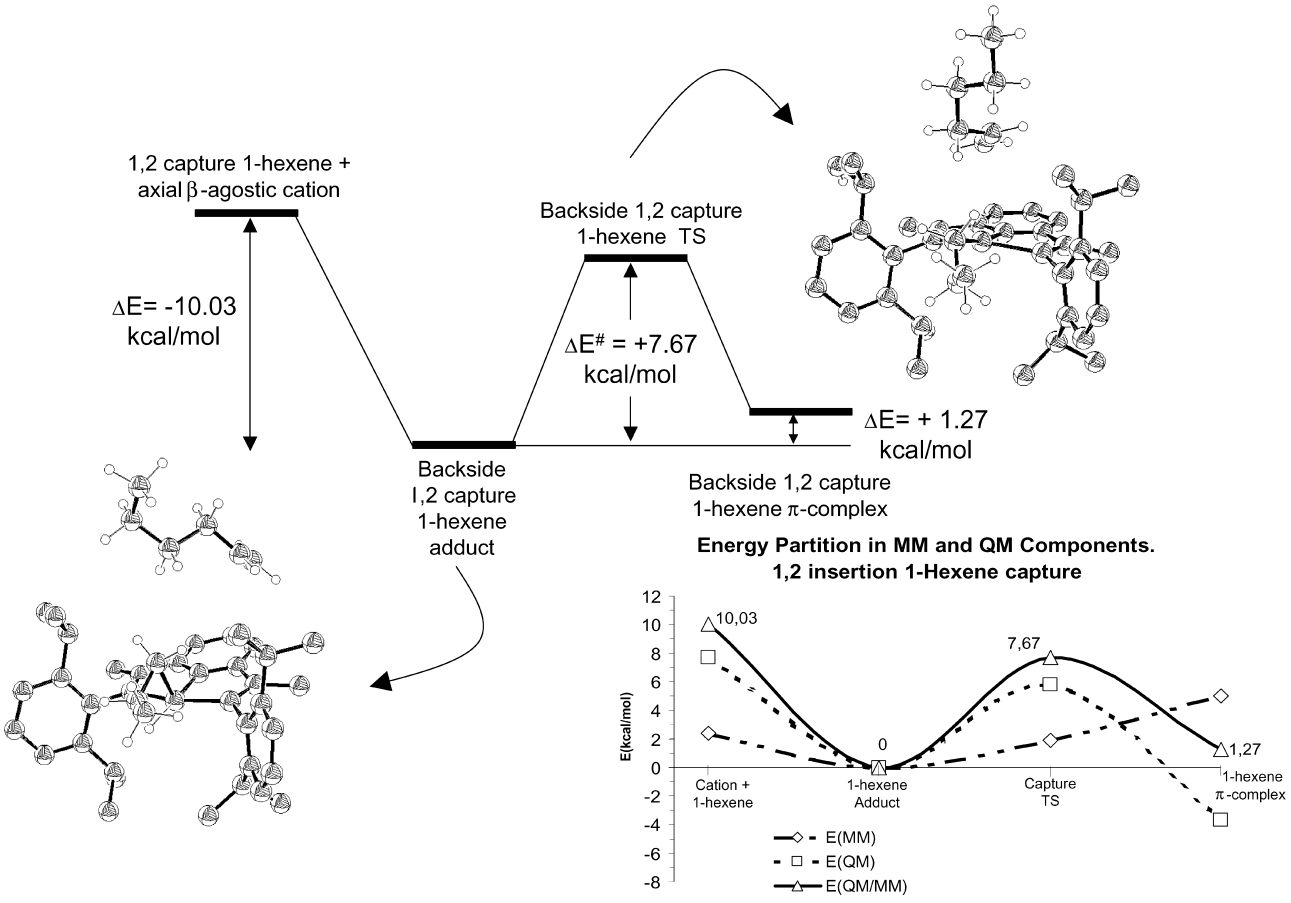

Fig. 7. Energy profile and $E_{QM/MM}$ partition for the propagation reaction of the 1-hexene in 1,2 form into the Fe–Cα bond.

easier than the 1-hexene capture by 4.51 kcal/mol. In addition, the 1-hexene π-complex formation is an endothermic step by 0.72 kcal/mol, while the ethylene π-complex is exothermic by 3.61 kcal/mol. Therefore, the axial backside 1-hexene capture is very unlike to occur if one compares this with a similar process for the ethylene monomer.

In the next reaction step, the π-complex progresses through the corresponding insertion transition state to the γ-agostic insertion product. Ethylene insertion occurs with a small energy barrier of 0.59 kcal/mol, while the 1-hexene has an insertion energy barrier of 5.43 kcal/mol.

We can then conclude that for both monomers the rate-limiting step for the olefin polymerisation with bisimine-pyridine catalysts based on iron metal seems to be the monomer capture rather the insertion step which is in close agreement with the published results by Deng et al. [43].

In summary, the ethylene propagation reaction is very favourable when it is compared with the 1-hexene. This is in good agreement with the experimental results that show the formation of the ethylene homopolymer rather ethylene/1-hexene copolymers.

In order to further clarify the propagation mechanism we have investigated in more detail the energy partition for the E_{MM} and E_{QM} components for the ethylene and 1-hexene capture and insertion steps. As can be seen in Fig. 6(a) the MM energy for the ethylene monomer which takes into account the ancillary ligands contributes to a decrease in the energy barrier for both the capture transition and insertion transition state making it more feasible the propagation step. This could be attributed to the attractive Van der Waals interactions between ethylene and ancillary ligands promoted by the small size of the ethylene molecule. On the contrary, the MM energies for the 1-hexene capture and insertion steps (Fig. 6(b)) increase the energy barriers of the transition states for both steps making more difficult the propagation step for this monomer. Additionally, the 1-hexene π-complex is less stable that the 1-hexene adduct due to the MM contribution. This could be caused by the repulsive Van der Waals interactions between the bulky 1-hexene monomer and the ancillary ligands.

It was mentioned earlier that the 2,1 insertion of 1-hexene is more probable that the 1,2 insertion. In Fig. 7 the energy profile and energy partition in MM and QM components of the capture process for 1,2 insertion of 1-hexene are shown. As it can be observed (compare Figs. 7 and 6(b)) due to the steric effects the 1,2 insertion is more unfavourable than the 2,1 insertion changing the capture energy barrier from 6.62 kcal/mol for 2,1 insertion to 7.67 kcal/mol for 1,2 insertion. Additionally, the destabilisation of the 1-hexene π-complex with respect to the 1-hexene adduct is

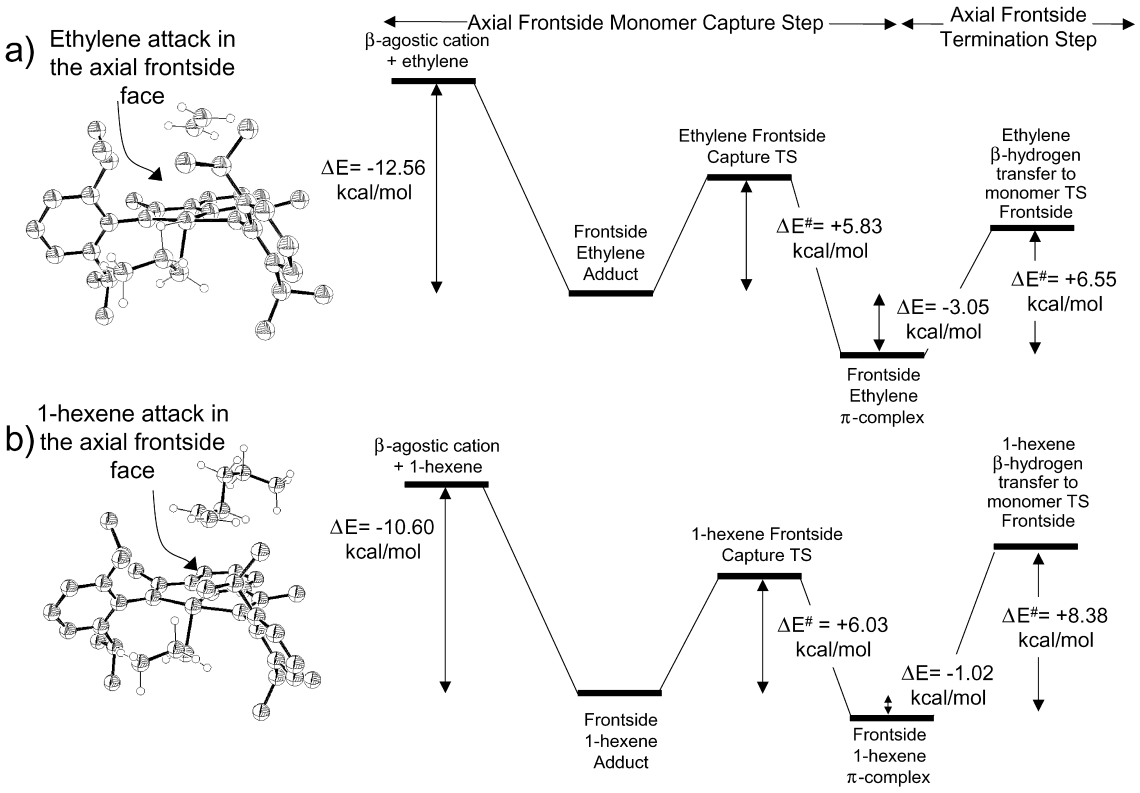

Fig. 8. Energy profile for the termination reaction (a) for ethylene (b) for 1-hexene monomers.

1.27 kcal/mol for 1,2 insertion versus 0.72 kcal/mol for 2,1 insertion. In conclusion, in a hypothetical homopolymerisation of 1-hexene the 2,1 insertion is more favourable than the 1,2 insertion. This latter observation is in close agreement with the experimental results reported by Brookhart's group [41], where they claim that the 2,1 insertion for propene polymerisation is more favourable than the 1,2 insertion.

3.4. Axial frontside monomer capture

As it was pointed out earlier, the axial frontside monomer capture brings the chain to a termination reaction via β-hydrogen transfer to the monomer. The axial frontside profiles for the ethylene and 1-hexene monomers are displayed in Fig. 8. The frontside capture step barrier for the ethylene is 5.83 kcal/mol and the termination step barrier is 6.55 kcal/mol. Thus, the rate-limiting step for the chain termination reaction is the β-transfer to the monomer rather than the frontside ethylene capture step. These energy barriers are higher than those corresponding to the capture and insertion in backside position (2.11 and 0.59 kcal/mol, respectively, see Fig. 4). The difference between the rate-limiting steps of the propagation (2.11 kcal/mol) and the termination processes (6.55 kcal/mol) is 4.44 kcal/mol. This value is close to the experimental estimation in the range of 4.0–6.0 kcal/mol for the difference between energy barriers for termination and propagation processes [38–41].

For the 1-hexene monomer the frontside capture barrier is 6.03 kcal/mol and the termination barrier 8.38 kcal/mol. The frontside capture barrier is slightly lower than the backside capture barrier (6.03 versus 6.62 kcal/mol) by 0.59 kcal/mol, being indicative of a favourable frontside capture versus a backside capture. In addition, the frontside π-complex formation is an exothermic step by 1.02 kcal/mol. This makes a difference with the backside capture where the backside π-complex formation is an endothermic process by 0.72 kcal/mol. In this case, the difference between the energy barriers for the propagation (+6.62 kcal/mol) and termination (+8.38 kcal/mol) reactions is only 1.76 kcal/mol.

Similarly, in order to clarify in more detail the mechanism of the termination reaction, the energy partition for the E_{MM} and E_{QM} components for the ethylene and 1-hexene frontside capture and β-H transfer to monomer steps have been analysed. As it can be seen in Fig. 9 for both monomers the energy barriers associated with the termination reaction are due mainly to the presence of the ancillary ligands that increases the frontside capture and the β-H transfer to monomer steps. Therefore, an important contribution of the ancillary ligands to the ethylene polymerisation is to increase the termination barriers and decrease the propagation barriers, so that a polymer is formed. In the case of 1-hexene monomer both the termination and propagation

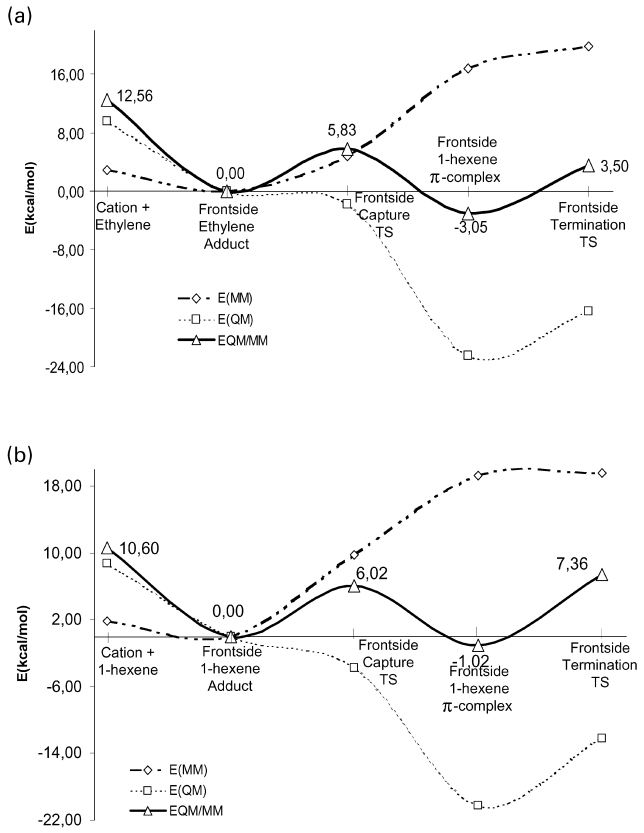

Fig. 9. Energy partition in MM and QM Components for the termination reaction of (a) ethylene (b) 1-hexene.

barriers are increased in such a way that the difference between them is smaller. Consequently, in a hypothetical 1-hexene homopolymerisation, low activities and low molecular weight polymers are to be expected.

4. Conclusions

From the above discussed results we can conclude the following remarks:

1. Two conformations for the alkyl cation species have been found: the equatorial and the axial conformation. The axial conformation of the alkyl cation species is the most stable by 16.33 kcal/mol. Therefore, it is supposed that the polymerisation process occurs from the axial conformation as reported by Deng et al. [43].
2. The monomer insertion in the equatorial plane is not a favourable process for this catalyst due to the very high-energy barriers for the ethylene and 1-hexene insertions (+31.52 and +36.15 kcal/mol, respectively). Additionally, these high barriers values are in clear disagreement with the experimental results that show a high activity of these catalysts during the ethylene polymerisation [38–41]. For this reason, one can conclude that the monomer insertion in the propagation cannot take place in the equatorial plane. As an alternative the monomer insertion in the axial position is proposed.
3. The energy barriers for the ethylene and 1-hexene propagation reactions are 2.11 and 6.62 kcal/mol for the capture step and 0.59 and 5.43 kcal/mol for the insertion step, respectively. For both monomers the rate-limiting step for the propagation mechanism is the backside monomer capture. From the above energy barriers, we can conclude that the ethylene propagation reaction is very favourable as compared to the 1-hexene propagation. This is in good agreement with the experimental results that shows the formation of ethylene homopolymer rather than ethylene/1-hexene copolymers.
4. The energy barriers for the ethylene and 1-hexene terminations are 5.83 and 6.03 kcal/mol for the frontside capture step and 6.55 and 8.38 kcal/mol for the frontside β-H transfer to monomer step, respectively. The difference between the rate-limiting step of the propagation process and the rate-limiting step of the termination step is 4.44 kcal/mol for the ethylene and is only 1.76 kcal/mol for the 1-hexene. This is an indication of an easy polymerisation process for the ethylene when compared to the 1-hexene monomer. Based on these calculations, low activities and low molecular weight polymer should be expected in a hypothetical 1-hexene homopolymerisation.
5. For the 1-hexene the 2,1 insertion is more probable than the 1,2. This is in good agreement with the experimental results reported by Brookhart's group for the propylene polymerisation.
6. The ancillary ligands play a very important role in the polymerisation activities and the resulting molecular weights. In the ethylene polymerisation, the propagation energy barrier decreases while the termination energy barrier increases yielding as result both higher activity and molecular weight. On the other hand, for 1-hexene polymerisation both the propagation energy barrier and the termination barrier increase in such a way that the overall activity and molecular weight decrease.

Acknowledgements

Thanks are due to the CICYT (Grant MAT99-1053) for the support of this investigation. One of us (J.R.) wishes to thank CICYT for the tenure of a fellowship. The authors also acknowledge Repsol-YPF for the permission to publish these data.

References

[1] Kaminsky W, Sinn H. Transition metals and organometallics for catalysts for olefin polymerisation. New York: Springer, 1988.
[2] Soares JBP, Hamielec AE. Polym React Engng 1995;117:3008.
[3] Brintzinger HH, Fischer D, Mülhaupt R, Rieger B, Waymouth RM. Angew Chem Int Ed Engl 1995;34:1143.

[4] Kaminsky W. Pure Appl Chem 1998;70(6):1229.
[5] Meier RJ, Van Doremaele GHJ, Iarlori S, Buda F. J Am Chem Soc 1994;116:7274.
[6] Margl P, Lohrentz JCW, Ziegler T, Blöchl PE. J Am Chem Soc 1996;118:4434.
[7] Lohrentz JCW, Woo TK, Ziegler T. J Am Chem Soc 1995;117:12793.
[8] Lohrentz JCW, Woo TK, Fan L, Ziegler T. J Organomet Chem 1995;497:91.
[9] Yoshida T, Koga N, Morokuma K. Organometallics 1995;14:746.
[10] Woo TK, Fan L, Ziegler T. Organometallics 1994;13:2252.
[11] Kawamura-Kuribayashi H, Koga N, Morokuma K. J Am Chem Soc 1992;114:8687.
[12] Cruz VL, Muñoz-Escalona A, Martínez-Salazar J. Polymer 1996;37:1663.
[13] Cruz VL, Muñoz-Escalona A, Martínez-Salazar J. J Polym Sci A: Polym Chem 1998;36:1157.
[14] Woo TK, Margl PM, Lohrenz JCW, Blöchl PE, Ziegler T. J Am Chem Soc 1996;118:13021.
[15] Muñoz-Escalona A, Ramos J, Cruz V, Martínez-Salazar J. Polymer 2000;38:571.
[16] Ramos J, Cruz V, Muñoz-Escalona A, Martínez-Salazar J. Polymer 2000;41:6161.
[17] Stevens JC, Timmers FJ, Wilson DR, Schmidt GF, Nickias PN, Rosen RK, Knight GW, Lai S. European Patent Application EP-416-815-A2; March 13,1991.
[18] Shapiro PJ, Bunel E, Schaefer WP, Bercaw JE. Organometallics 1990;9:867.
[19] Fan L, Harrison D, Woo T, Ziegler T. Organometallics 1995;14:2018.
[20] Mack H, Eisen MS. J Chem Soc, Dalton Trans 1998;6:917.
[21] Herskovics-Korine D, Eisen MS. J Organomet Chem 1995;503:307.
[22] Littke A, Sleiman N, Bensiman C, Richeson DS, Yap GPA, Brown SJ. Organometallics 1998;17:446.
[23] Ramos J, Muñoz-Escalona A, Cruz V, Martínez-Salazar J. Polymer 2001;42:7275.
[24] Johnson LK, Killian CM, Brookhart M. J Am Chem Soc 1995;117:6414.
[25] Killian CM, Tempel DJ, Johnson LK, Brookhart M. J Am Chem Soc 1996;118:11664.
[26] Ittel SD, Jonson LK, Brookhart M. Chem Rev 2000;100:1169.
[27] Johnson LK, Mecking S, Brookhart M. J Am Chem Soc 1996;118:267.
[28] Deng L, Margl PM, Ziegler T. J Am Chem Soc 1997;119:1094.
[29] Musaev DG, Froese RDJ, Svensson M, Morokuma K. J Am Chem Soc 1997;119:367.
[30] Musaev DG, Froese RDJ, Morokuma K. New J Chem 1997;21:1269.
[31] Strömberg S, Zetterberg K, Siegbahn PEM. J Chem Soc, Dalton Trans 1997;22:4147.
[32] Musaev DG, Morokuma K. Top Catal 1997;119:367.
[33] Deng L, Woo TK, Cavallo L, Margl PM, Ziegler T. J Am Chem Soc 1997;119:6177.
[34] Woo TK, Ziegler T. J Organomet Chem 1999;591:204.
[35] Froese RDJ, Musaev DG, Morokuma K. J Am Chem Soc 1998;120:1581.
[36] Musaev DG, Froese RDJ, Morokuma K. Organometallics 1998;17:1850.
[37] Ramos J, Muñoz-Escalona A, Cruz V, Martínez-Salazar J. Polymer 2001;42(19):8019.
[38] Small BL, Brookhart M, Bennet AMA. J Am Chem Soc 1998;120:4049.
[39] Britovsek GJP, Gibson VC, Kimberley BS, Maddox PJ, McTavish SJ, Solan GA, White AJP, Williams DJ. Chem Commun 1998:849.
[40] Britovsek GJP, Bruce M, Gibson VC, Kimberley BS, Maddox PJ, Mastroianni S, McTavish SJ, Redshaw C, Solan GA, Strömberg S, White AJP, Williams DJ. J Am Chem Soc 1999;121:8728.
[41] Small BL, Brookhart M. Macromolecules 1999;32:2120.
[42] Griffiths EAH, Britovsek GJP, Gibson VC, Gould IR. Chem Commun 1999:1333.
[43] Deng L, Margl P, Ziegler T. J Am Chem Soc 1999;121:6479.
[44] ADF User's Guide. ADF Program System Release 2000.02.
[45] Maseras F, Morokuma K. J Comput Chem 1995;16:1170.
[46] Woo TK, Caballo L, Ziegler T. Theor Chem Acc 1998;100:307.
[47] Vosko H, Wilk L, Nusair M. Canadian J Phys 1980;58:1200.
[48] Becke AD. Phys Rev A 1988;38:3098.
[49] Perdew JP. Phys Rev B 1986;33(12):8822.